Performance of the thin film coating on the long and collimating BEaTriX parabolic mirror

Nis Christian Gellert[a],* **Sonny Massahi[a]** **Bianca Salmaso[b]**
Daniele Spiga[b] **Desiree Ferreira[a]** **Gabriele Vecchi[b]** **Ivo Ferreira[c]**
Marcos Bavdaz[c] **Stefano Basso[b]** **Sara Svendsen[a]** **Arne S Jegers[a]** and
Finn E. Christensen[a]

aTechnical University of Denmark (DTU Space), Lyngby, Denmark
bINAF-Osservatorio Astronomico di Brera, Merate, Italy
cEuropean Space Agency, ESTEC, Noordwijk, The Netherlands

Abstract. Long mirrors coated with thin films are used for a wide range of applications, e.g., focusing or collimating high-energy optics. Focusing of incident x-ray radiation is one of the major applications for high-energy astronomical telescopes, and collimation of divergent x-ray sources is used for experimental setups to confine or expand x-ray radiation. Both applications utilize grazing angle reflection, which is typically enhanced using x-ray reflective thin films. One of the challenges with thin film coatings is the deposition induced nonuniformities. For x-ray reflecting mirrors, nonuniformity in the thin film deposition influences the thickness, roughness, and density of the thin film, which affects the predicted performance of the mirror. As part of the thin film coating development for the 456-mm-long parabolic mirror used in the Beam Expander Testing X-ray facility, our work presents the challenge of coating long x-ray reflective mirrors. We used x-ray reflectometry to investigate the nonuniformity in platinum and chromium thin films deposited using direct current magnetron sputtering. © *The Authors. Published by SPIE under a Creative Commons Attribution 4.0 International License. Distribution or reproduction of this work in whole or in part requires full attribution of the original publication, including its DOI.* [DOI: 10 .1117/1.JATIS.9.2.024004]

1 Introduction

The BEaTriX (Beam Expander Testing X-ray[1–3]) facility is the laboratory located at INAF-OAB (Italian National Institute for Astrophysics, Brera Astronomical Observatory[4]). The BEaTriX facility was commissioned to characterize the silicon pore optics (SPO)[5] modules of the Advanced Telescope for High-ENergy Astrophysics[6,7] x-ray observatory. The facility will operate at the monochromatic x-ray energies of 4.511 and 1.487 keV, using a titanium and aluminium x-ray microfocus source, placed at the focus of a grazing incidence parabolic mirror. The 4.511 keV beam line is operational, and the 1.487 keV beam line will be implemented in the coming months. The 456-mm-long parabolic mirror is designed to ensure collimation and uniformity to the beam. The parabolic mirror substrate is made of heraeus optical quality (HOQ) 310 fused quartz (SiO$_2$) with the specifications as presented in Fig. 1. The 10-mm area along the edges of the parabolic surface have no optical requirements. The parabolic mirrors' operating incidence grazing angle is 0.9 deg. The collimated beam reflected by the mirror is 4 mm wide and 60 mm high. The reflected beam is then monochromated by four symmetrically cut silicon (Si) crystals, isolating the $K - \alpha$ fluorescence line of the x-ray source at 4.511 keV. The beam is finally expanded in the horizontal direction by an asymmetrically cut Si crystal. The final beam size is 170 mm × 60 mm, which enables full illumination of the SPO mirror modules. With this setup, the BEaTriX facility is characterized to have a horizontal x-ray beam divergence between 2.7 and 3.45 arcsec and a vertical divergence of 1.65 arcsec.[3,9]

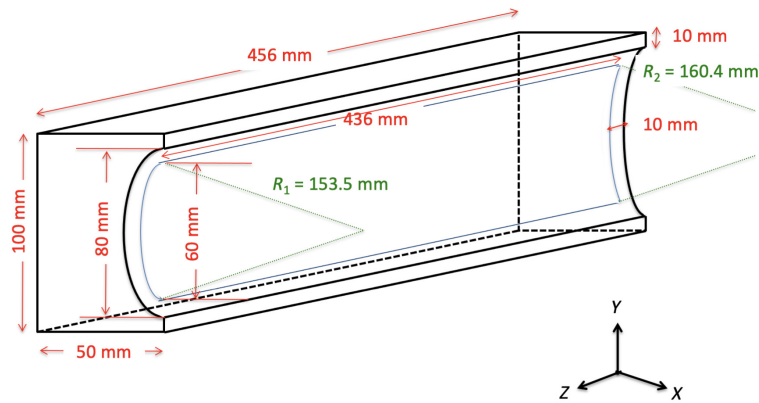*Address all correspondence to Nis Christian Gellert, nige@space.dtu.dk

Fig. 1 Sketch of the BEaTriX parabolic mirror design.[8]

To increase the reflectivity at 4.511 keV, the 456-mm-long parabolic mirror is coated with platinum (Pt) due to its high density, which enhances the grazing incidence reflection. For this reason, Pt is utilized in the reflective coating optics for the x-ray telescopes Nuclear Spectroscopic Telescope Array[10] and Astro-H.[11]

One of the disadvantages of Pt is that the Pt films have poor adhesion properties on SiO_2 because Pt easily reacts with Si and forms a platinum silicide, which can lead to delamination and time-dependent performance deterioration.[12,13] A thin intermediate layer of chromium (Cr) deposited between the parabolic mirror substrate and the Pt layer can be used to enhance the adhesion of the Pt layer. Cr is often used as an adhesion layer in several applications due to its high binding strength with oxygen, and it can therefore be used as the interconnecting layer between the substrate and coating material. Cr is utilized for such properties on the Chandra x-ray Observatory.[14] However, Cr thin films are known to exhibit a high surface roughness, and therefore it is important that the Cr does not affect the performance of the parabolic mirror. With the large size of the parabolic mirror, a coating nonuniformity is expected across the beam direction of the mirror that is due to the geometry of the direct current (DC) magnetron coating facility at Technical University of Denmark (DTU Space), causing possible reduction of the reflectivity if the coating thickness is reduced below the nominal value of 30 nm. In this paper, we evaluate the nonuniformity in the 456-mm-long mirror and the effect on the Pt surface roughness when introducing Cr as an adhesion layer.

2 Coating Design Considerations

The coating structure is designed by INAF-OAB and consists of 30 nm Pt with a 4 to 5 nm intermediate Cr layer. The Pt coating is necessary for the parabolic mirror to enhance the system performance at 4.511 keV. This is illustrated in Fig. 2, as the reflectivity for SiO_2 at 4.511 keV is $<10^{-2}$.

With the relatively large length (456 mm) of the parabolic mirror, a considerable nonuniformity in the coating thickness and roughness is expected across the beam direction of the mirror, and it should be minimized. There will be different target-substrate distances (TSD) seen by the mirror due to the geometry of the DC magnetron coating facility at DTU Space, resulting in different deposition rates across the mirror. The mirror will be mounted on a rotating ring, and therefore different angles of incidence of the sputtered material are inevitable, which is reported to increase the roughness and decrease the density toward the mirror edge related to columnar growth.[15–17] A vertical nonuniformity is also considered, but past studies and additional investigations have shown that the relatively small 60 mm height and large radius of curvature will not affect the vertical coating uniformity.[18] The coating chamber geometry and three mirror positions are illustrated in Fig. 3. Assuming that the deposition follows a straight line drawn perpendicular to the center of the target, it is illustrated that the TSD will fluctuate during the mirror thin film deposition, and the perpendicular TSD is expressed as
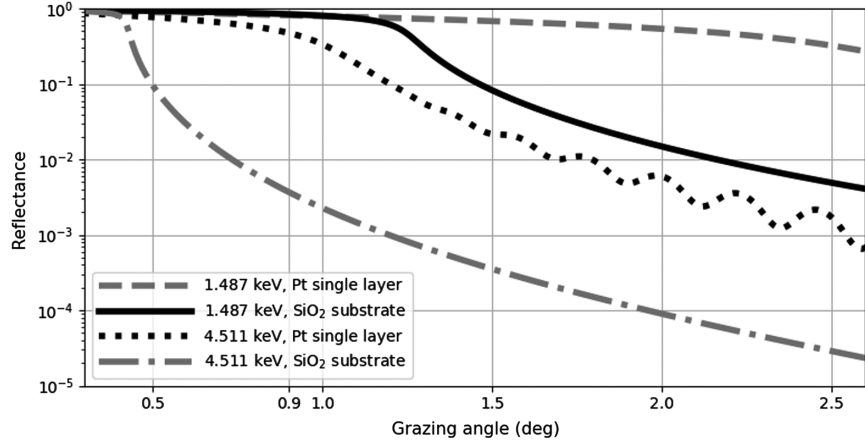
Fig. 2 Simulated reflectance of a SiO_2 substrate and a 30 nm Pt single layer on a SiO_2 substrate at 1.487 keV and 4.511 keV. A 0.4 nm roughness is used for the simulations.
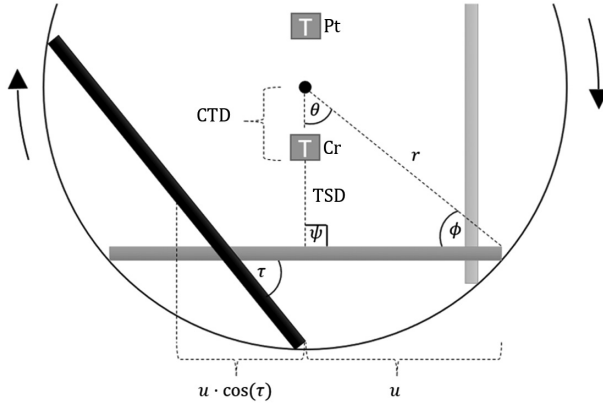

Fig. 3 Illustration of the DTU coating chamber seen from above, with parabolic mirror during pre-sputter (light gray), directly across from the fixed Cr target T (dark gray), and rotated (black) such that the edge of the mirror is in front of the target, so the mirror is tilted with an angle τ relative to the mirror position directly across the target. The parabolic mirror is assumed to be flat in the beam direction. The illustration is not to scale.

$$\text{TSD} = \frac{r \sin(\phi)}{\sin(\psi)} - \text{CTD}. \tag{1}$$

When the mirror is directly across from the fixed target (T), the shortest $\text{TSD}_{\min} = 94$ mm, and

$$\theta_{\min} = \arcsin\left(\frac{u}{r}\right), \tag{2a}$$

$$\psi_{\min} = \frac{\pi}{2}, \tag{2b}$$

$$\phi = \pi - \theta_{\min} - \psi_{\min}, \tag{2c}$$

where u is half the mirror length and the distance r from the center of the chamber to the edge of the mirror surface is given by

$$r = \sqrt{(\text{TSD}_{\min} + \text{CTD})^2 + u^2}, \tag{3}$$

where CTD = 273 mm is the distance from the center of the chamber to the target surface. When the mirror has rotated such that the edge of the mirror is in front of the target, so that the mirror is tilted with an angle τ relative to the mirror position directly across the target, the longest TSD is calculated as TSD_{max} = 159 mm. Assuming that the deposition rate reduction follows a simple inverse square law dependency, the horizontal deposition rate nonuniformity (T_z) is expressed as

$$T_z = \cos(\tau_{max}) \frac{(TSD_{min})^2}{(TSD_{max})^2}. \tag{4}$$

The TSD is increased by 65 mm at the edge of the mirror, and the maximum tilted angle is roughly τ_{max} = 32 deg, yielding a 70% reduction in the deposition rate at the edge. This will give a thickness of 9 nm at the edge of the BEaTriX mirror. It must be noted that the model does not take the solid angle of sputtered particles into account, which may increase the actual thickness. Figure 4 illustrates the effect of a 20% and 60% reduction in the Pt thickness at 4.511 keV. It is shown that the thickness reduction does not change the reflected intensity at 0.9 deg. A thickness variation across the parabolic mirror will therefore not affect the BEaTriX beam's efficiency. However, Pt has poor adhesion properties,[13] and adhesion can be enhanced by an intermediate Cr protective coating between the substrate and Pt film. Cr thin films are known to contribute to a high surface roughness due to their grainy growth during deposition, and therefore it is important that the Cr does not affect the interface roughness or Pt surface roughness. Massahi et al.[19] reported on an investigation regarding the balancing of the residual stress in iridium (Ir) thin films by utilizing Cr as an underlayer and found that the Ir surface roughness slightly increases with the Cr thickness. Furthermore, the increasing angle τ of the sputtered material onto the mirror is reported to increase the roughness, which may be related to columnar growth. The largest grazing deposition angle is τ_{max} = 32 deg, and Dalla Torre et al.[16] reported on tantalum films sputtered onto inclined substrates and showed that the roughness increased by >100% at 60 deg. Figure 4 includes two models of a Pt single layer with higher surface roughnesses. It shows that a 100% to 225% increase in surface roughness will affect the reflected intensity at 0.9 deg by 8% to 19%.

Due to the geometric structure and current equipment drive systems of the DC magnetron coating facility, it is currently not possible to deposit a thin film with a uniform coating thickness across the beam direction of the mirror substrate. A nonuniformity in the deposited thickness is expected, but it is shown that the thickness nonuniformity will not affect the predicted performance of the mirror. However, it is critical for the BEaTriX system performance to investigate the effect of using Cr as an intermediate layer to avoid delamination of Pt and if the interfacial roughness will be affected by different TSDs seen by the mirror and varying incidence of the sputtered material.
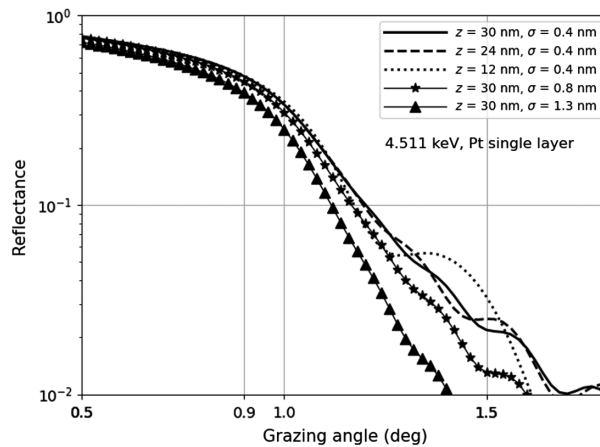

Fig. 4 Simulated 4.511 keV model of a nm Pt single layer on a SiO$_2$ substrate, to be compared with 20% and 60% thickness (z) decreases. The effect of increased Pt surface roughness (σ) is included.

Table 1 Samples and associated coating designs in each study. The expected thicknesses in the nonuniformity study were calculated using Eq. (4).

Study	Sample ID	Material	Expected center thickness (nm)
	ds0008	Pt	30.0
Surface roughness	ds0021	Cr/Pt	5.0/30.0
	ds0027	Cr/Pt	2.5/30.0
	Parabolic mirror	Cr/Pt	5.0/30.0
	ds0077	Cr/Pt	1.5/9.0
Nonuniformity	ds0078	Cr/Pt	3.3/20.0
	ds0079	Cr/Pt	5.0/30.0
	ds0080	Cr/Pt	3.3/20.0
	ds0081	Cr/Pt	1.5/9.0

3 Experimental Procedure

3.1 Sample Preparation

This paper consists of two studies: the surface roughness and the nonuniformity. The thin films presented were produced at the DC magnetron sputtering facility at DTU Space.[20] We deposited the thin films onto double-side polished Si substrates, referred to as witness samples, with a crystal orientation (100) and dimensions of 70 mm × 10 m × 0.775 mm ($L \times W \times H$). Three samples were used to evaluate the Pt surface roughness when introducing Cr as an adhesive layer: one Pt single layer and two Cr/Pt bilayers, as listed in Table 1. Due to the parabolic mirror's large size and the sample size limitation on our x-ray reflectometry equipment, it was not possible to measure the thin film coating nonuniformity on the parabolic mirror. A reference coating was therefore performed after the mirror coating with the same deposition parameters, which included 5 witness samples divided across 456 mm, as listed in Table 1. All witness sample substrates were plasma cleaned prior to the thin film deposition, with a power of 100 W for 40 min in an oxygen (O_2)/nitrogen (N_2) atmosphere using a Tepla Plasma Asher. The parabolic mirror was polished at INAF-OAB[9] before arrival at DTU Space, and a visual inspection showed no defects or surface particles. Before the parabolic mirrors thin film deposition, the surface was cleaned using a N_2 gun to remove dust and other particulates from the substrate surface.

During the thin film deposition, we applied a power density of 1.55 W/cm^2 to the Pt target and 2.33 W/cm^2 to the Cr target. We preconditioned the Pt and Cr targets for 5 min to remove impurities from the target surface and performed all coatings in an argon atmosphere with a pressure of 3.0 mTorr. The BEaTriX parabolic mirror is placed in the center of a custom-built mirror mounting plate, shown in Fig. 10, and the 5 reference samples' relative locations across the 456 mm are illustrated in Fig. 5. The aimed thicknesses of each sample is listed in Table 1. The reference samples were mounted on a 50-mm-tall plate to achieve the same TSD as for the parabolic mirror and rotated around the magnetron during the coating process using calibrated ring rotation speeds. The parabolic mirror was coated with a center TSD of 94 mm and mirror edge TSD of 159 mm, using a collimating honeycomb mesh[15] in front of the target.

3.2 X-ray Reflectometry Characterization

X-ray reflectometry measurements at 1.487 keV were performed with the low-energy x-ray reflectometer (LEXR[21]) at DTU Space and 8.048 keV measurements using the Rigaku SmartLab X-Ray Diffractometer at DTU Nanolab. Energy scans were measured at the
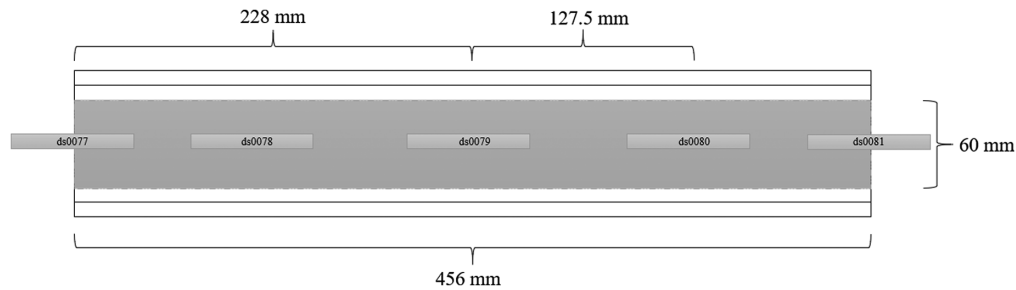
Fig. 5 Reference sample location, samples ds0077 to ds0081.

four-crystal monochromator beamline of the Physikalisch-Technische Bundesanstalt laboratory at the BESSY II synchrotron radiation facility,[22] though these results will be shown in later work.

Specular ($\theta - 2\theta$) and nonspecular (θ) measurements were conducted using the 1.487 keV reflectometer. For both measurements, the reflectometer was operated with a 0.5×1.0 mm^2 ($W \times H$) beam shaping slit. The sample to source distance was 1485 mm, and the sample to detector distance was 504 mm. For the specular measurements, a 4.0×5.0 mm^2 ($W \times H$) slit was used to filter out undesired scattering before the resulting beam intensity was recorded. For the nonspecular measurements, the detector stage was fixed at 2θ while scanning the sample in the interval $\theta = [0,2\theta]$ with a 1.0×5.0 mm^2 ($W \times H$) detector slit. The 8.048 keV reflectometer at DTU Nanolab has a sample to detector distance of 351.4 mm and uses a 0.12×2.0 mm^2 ($W \times H$) detector slit to shape the beam reaching the sample, and the width of the slit after sample reflection was 1.87 mm. The measured reflectometry data were fitted using a Python-based software that utilizes the Fresnel equations in combination with a differential evolution algorithm, as described in Gellert et al.[23] The optical constants for each material is computed using the atomic scattering factors from the Center for X-Ray Optics.[24] An angular instrumental resolution of 0.007 deg is specified for the 8.048 and 1.487 keV system. All model structures were composed of a Si substrate with a native SiO$_2$ surface. The SiO$_2$ thickness was fixed at 2.0 nm (the typical value for native grown oxide[20]), and the roughness was coupled to that of the Si substrate. For the 1.487 keV models, we introduced an overlayer of hydrocarbons (C−H−O) with a density fixed to 1.0 g/cm^3, which accounts for any C−H−O compound and other surface contaminants visible at 1.487 keV, as presented by Massahi et al.[25] The roughness of the C−H−O overlayer is coupled to the underlying Pt roughness because this parameter cannot be constrained from the fit.

4 Results and Discussion

4.1 Surface Roughness

We show the effect of using Cr as an intermediate layer by conducting specular and nonspecular x-ray reflectometry measurements using the 1.487 keV reflectometer (LEXR) at DTU Space on the three samples listed in Table 1. We performed nonspecular measurements at 0.3 deg, 0.9 deg, and 2.5 deg. The nonspecular scan at 0.3 deg is compared with the technical report from INAF-OAB,[26] 0.9 deg due to being the facility's operating angle, and 2.5 deg due to being near the critical angle for Pt at 1.487 keV. All measurements are included in Fig. 6.

The 1.487 keV specular measurements including their best-fit models are shown in Fig. 7, and the best-fit parameters are given in Table 2. The widths of the fringes are well modeled, which is related to a good thickness estimate. We observe a very low residual, with the largest deviations being observed in the peaks and valleys of the Kiessig fringes, which may be due to a substrate waviness or a small film nonuniformity along the measurement direction.[25] The Cr layers' effect on the reflection process is observable near 9 deg. The 1.487 keV specular reflectivity measurements in Fig. 6 indicate that a thin intermediate layer of Cr does not affect the Pt surface roughness because the slope of the reflectance after the critical angle is similar for the three samples.
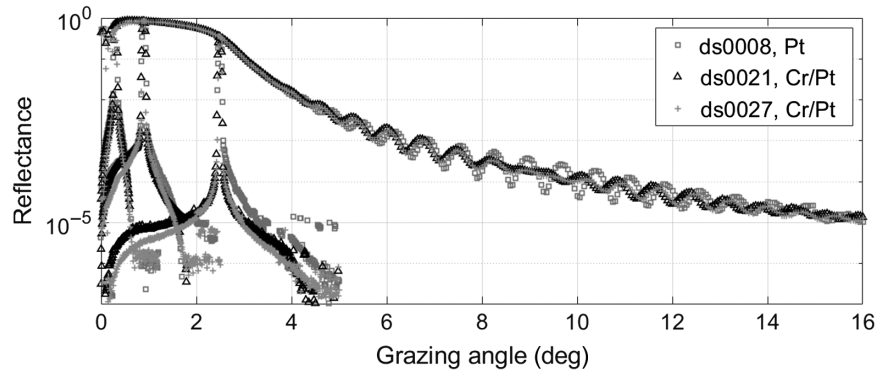
Fig. 6 Measured 1.487 keV specular and nonspecular reflectivity at 0.3 deg, 0.9 deg, and 2.5 deg of samples ds0008, ds0021, and ds0027.
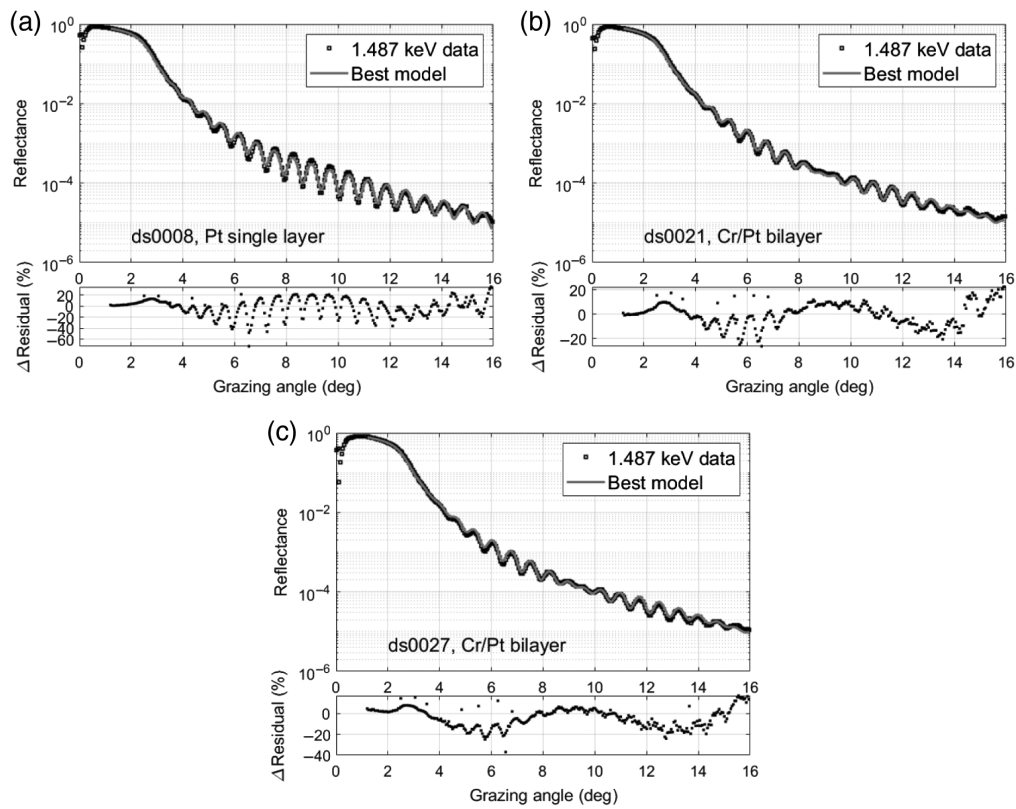

Fig. 7 1.487 keV specular reflectivity measurements of samples (a) ds0008, (b) ds0021, and (c) ds0027, including the best-fit model. Table 2 includes the fitted model parameters.

The best-fit parameters in Table 2 show that the Cr roughness is a factor of 2 higher compared with the Pt surface roughness, due to the grainy growth of the Cr thin film during deposition.[19] The surface roughness of the Pt film increased slightly (6.9%) when deposited on top of Cr due to the high Cr roughness. This trend is also reported by Massahi et al.[19] in a Cr/Ir bilayer structure, in which the Ir surface roughness increases with increasing the Cr thickness. The fitted model parameters show that the Pt thicknesses are within 8% of their aimed values, which is acceptable and under our estimated 10% DC magnetron thickness accuracy. We obtained an average Pt density that is 94% of bulk density[27] (21.5 g/cm³). The modeled Cr densities were 6.88 and 7.19 g/cm³ corresponding to 96% and 100% of the bulk density[27] (7.19 g/cm³), respectively. Different models were tested, which account for misalignment, but it did not

Table 2 Fitted model parameters of the 1.487 keV specular reflectivity measurements of samples ds0008, ds0021, and ds0027. Figure 8 includes the measured data and fitted model.

Sample ID	Energy (eV)	Layer	Composition	Thickness (nm)	Density (g/cm^3)	Roughness (nm)
ds0008	1487	Top	C–H–O	**1.7**	1.0[c]	0.28[a]
		Intermediate 2	Pt	**32.3**	**20.05**	0.28[a]
		Intermediate 1	SiO$_2$	2.0[c]	2.65[d]	0.43[b]
		Substrate	Si	—	2.33[d]	0.43[b]
ds0021	1487	Top	C–H–O	**1.6**	1.0[c]	0.30[a]
		Intermediate 3	Pt	**28.9**	**20.29**	0.30[a]
		Intermediate 2	Cr	**4.2**	**6.88**	**0.59**
		Intermediate 1	SiO$_2$	2.0[c]	2.65[d]	0.47[b]
		Substrate	Si	—	2.33[d]	0.47[b]
ds0027	1487	Top	C–H–O	**1.6**	1.0[c]	0.30[a]
		Intermediate 3	Pt	**28.7**	**20.11**	0.30[a]
		Intermediate 2	Cr	**3.9**	**7.19**	**0.57**
		Intermediate 1	SiO$_2$	2.0[c]	2.65[d]	0.49[b]
		Substrate	Si	—	2.33[d]	0.49[b]

[a]Coupled parameters.
[b]Coupled parameters.
[c]Fixed values based on a priori assumptions (described in text).
[d]The density of Si and native SiO$_2$.
[e]The parameters allowed to vary are presented in bold.

improve the fitted model. The average best-fit thickness of the C–H–O overlayers derived from the 1.487 keV x-ray reflectivity (XRR) data was 1.6 nm, which is in agreement with the range of values reported by Massahi et al.[19]

The normalized nonspecular measurements at 0.3 deg, 0.9 deg, and 2.5 deg are included individually in Fig. 8. The measurement at 0.3 deg agrees with the results from the INAF-OAB technical report,[26] which show that a thin intermediate layer of Cr decreases the nonspecular reflectance. The measurements at 0.9 deg and 2.5 deg also agree with this trend, showing that the Pt single layer exhibits a higher level of nonspecular scatter than the bilayers, which suggests higher roughness due to the poor adhesion of the Pt and consequent delamination. Note that the measurements are known as rocking curve or ω scans, with the detector stage being fixed at 2θ while scanning the sample in the interval $\theta = [0,2\theta]$. This explains the asymmetrical spectrum as each angle represents a different beam illumination area of the sample.

We performed a rudimentary tape test with transparent 3M Scotch tape to evaluate the adhesion on the witness samples. A piece of Scotch tape was firmly attached onto the surface of the coating for each sample and subsequently pulled off the surface. Then, a visual inspection of the surfaces was performed, and the Cr/Pt bilayer films showed no visible residual on the tape and proved to withstand the removal of the tape. As can be seen in Fig. 9, the Pt single layer displays a visible residual from delamination.

We can conclude that the surface roughness of the Pt film increased slightly when deposited on top of Cr due to the high Cr roughness. This slight roughness increase is however negligible in relation to how the thin intermediate Cr layer greatly improves the adhesion of Pt thin films. The reflectivity and smoothness of the Pt surface is not damaged by a thin Cr interface and, in fact, improves the nonspecular reflectance and effectively prevents delamination. These results favor the Cr/Pt bilayer mirror coating design.
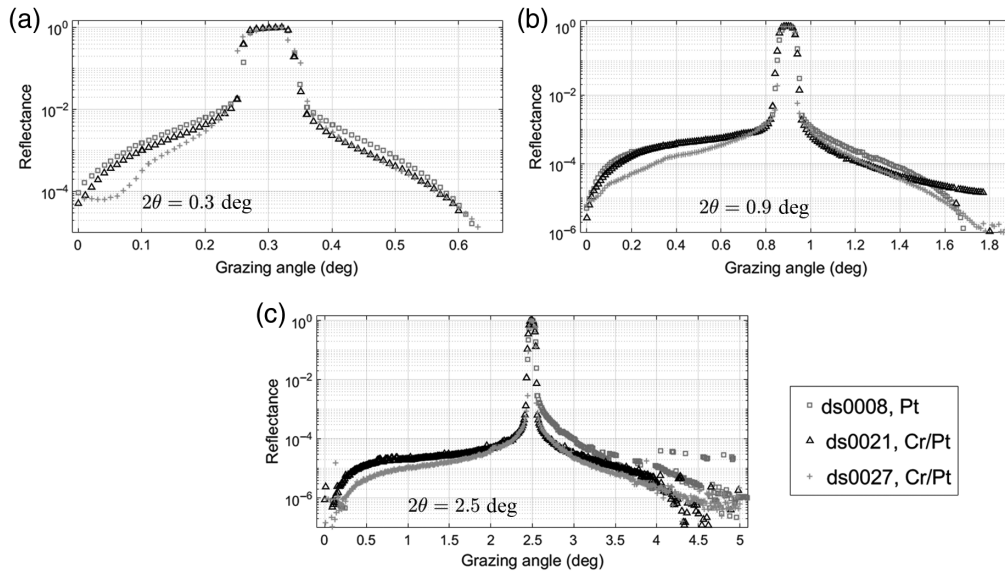
Fig. 8 Normalized 1.487 keV nonspecular reflectivity measurements at (a) 0.3 deg, (b) 0.9 deg, and (c) 2.5 deg of samples ds0008, ds0021, and ds0027.
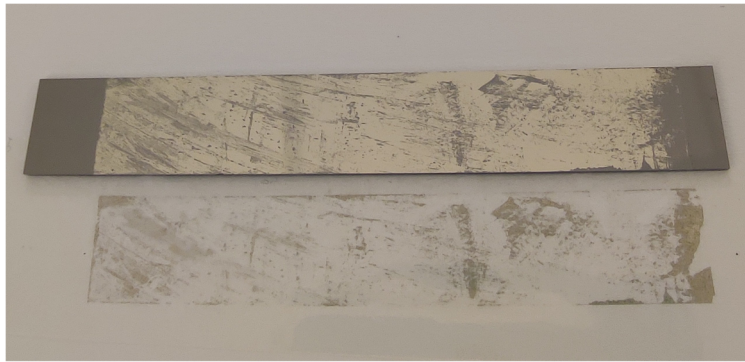

Fig. 9 Tape test on Pt single layer, sample ds0008.

4.2 Nonuniformity

Based on the previous results in Sec. 4.1, a center mirror coating consisting of 4 to 5 nm Cr + 30 nm Pt is chosen for the parabolic mirror. Due to the geometric structure and current equipment drive systems of the DC magnetron coating facility, it is currently not possible to deposit a thin film with a uniform coating thickness across the beam direction of the mirror substrate. We however showed in Sec. 2 that a 20% to 60% thickness reduction across the parabolic mirror did not affect the BEaTriX beam's efficiency, though the system performance was affected by the amount of scatter due to the roughness nonuniformity introduced by the varying TSD and incidence angle of the sputtered material. Therefore, as part of the thin film coating development for the 456-mm-long parabolic mirror, we evaluated the thickness and roughness nonuniformity along the length of the mirror. Figure 10 shows the parabolic mirror mounted in the chamber after coating. Due to the parabolic mirror's length and the sample size limitation on the available reflectometry equipment, it was not possible to measure the coated parabolic mirror. A reference coating was therefore performed after the parabolic mirror coating with the same deposition parameters, which included 5 witness samples divided across 456 mm, as illustrated in Fig. 5.

The 5 reference samples were measured by the 8.048 keV reflectometer at DTU Space, and the specular reflectivity measurements of samples ds0077 to ds0081, including their best-fit models, are shown in Fig. 11. It is observed that the specular reflectivity of samples ds0077
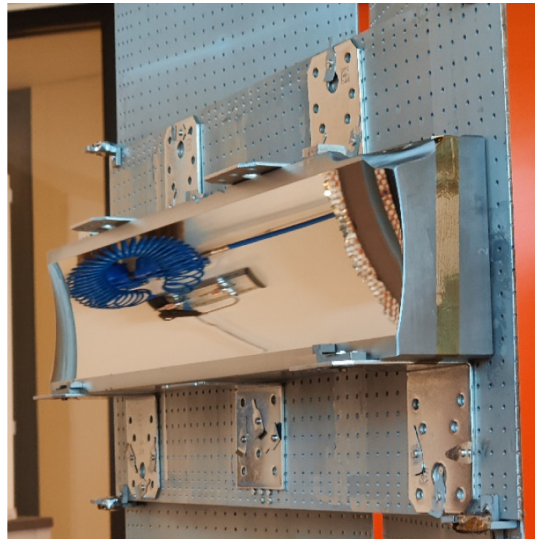
Fig. 10 Parabolic mirror mounted in the DC magnetron coating chamber after coating.

and ds0078 includes smeared features, indicating a larger roughness than the other samples. The data were analyzed and modeled as described in Sec. 3.2. Unlike the 1.487 keV XRR measurements, we did not fit the Cr and Pt densities to model the 8.048 keV XRR data obtained from the Cr/Pt bilayers. After preliminary attempts to model the Cr and Pt densities, these parameters could not be constrained, indicating an alteration in the samples model structures. We therefore used a Cr density of 7.19 g/cm^3 and a Pt density[19,27] of 21.5 g/cm^3. The best-fit parameters are shown in Table 3. The fitted model parameters show that the center sample ds0079 has a Pt thickness of 30 nm and the Cr thickness is 4.1 nm.

A uniformity map of the best-fit Cr and Pt thicknesses is shown in Fig. 12. The fitted Pt thickness shows a close to symmetric nonuniformity, in which the thickness decreases ~9% from the center to the midway and ~28% at the very edge of the mirror. The Cr thickness nonuniformity is not as symmetric, compared with the Pt thickness. The Cr thickness decreases between ~5% and 12% to the edge of the mirror. This nonsymmetric variation can be due the difficulty of sputtering and fitting Cr < 5 nm in a bilayer structure or may be attributed to the presputtering. Samples ds0077 and ds0078 may have been affected by the angular spread of particles from the Pt target during presputtering, despite not directly facing it. Samples ds0081 and ds0082 may correspondingly have been affected by the presputtering of the Cr target. This may explain the skewed Pt and Cr thickness nonuniformity of all samples and likely may be the reason for the unconstrained densities in the preliminary models. The coating contamination due to the large spread of particles from the magnetron has since been evaluated and confirmed, and new collimators are being designed for future use.

The measured Pt and Cr thicknesses are not consistent with the expected thicknesses when assuming that the deposition rate reduction follows a simple inverse square law dependency described by Eq. (4). This underestimation by a factor of two of the expected thickness as a function of rotation is due to the assumption of the target being 1D, and Eq. (4) does not account for the angular particle distribution.

The fitted roughnesses are included in Fig. 12. The roughness is expected to increase toward the edges due to the increased TSD and increasing angle of incidence of the sputtered particles onto the substrate. The fitted Pt roughnesses indicate a smooth surface uniformity of ~0.47 nm. The fitted Cr and substrate roughnesses support the notion that the observed results are due to the presputtering. The smeared features and high roughness of samples ds0077 and ds0078 can be explained by a thin Pt layer applied to the substrate during presputtering, causing a higher roughness due to the poor adhesion of the Pt. Disregarding samples ds0077 and ds0078, the fitted model parameters indicate a trend of increasing roughness toward the edge of the mirror, which is attributed to the increased TSD and the increasing angle of incidence of the sputtered particles. Vecchi et al.[9] reported that the parabolic mirror surface roughness slightly decreased after coating
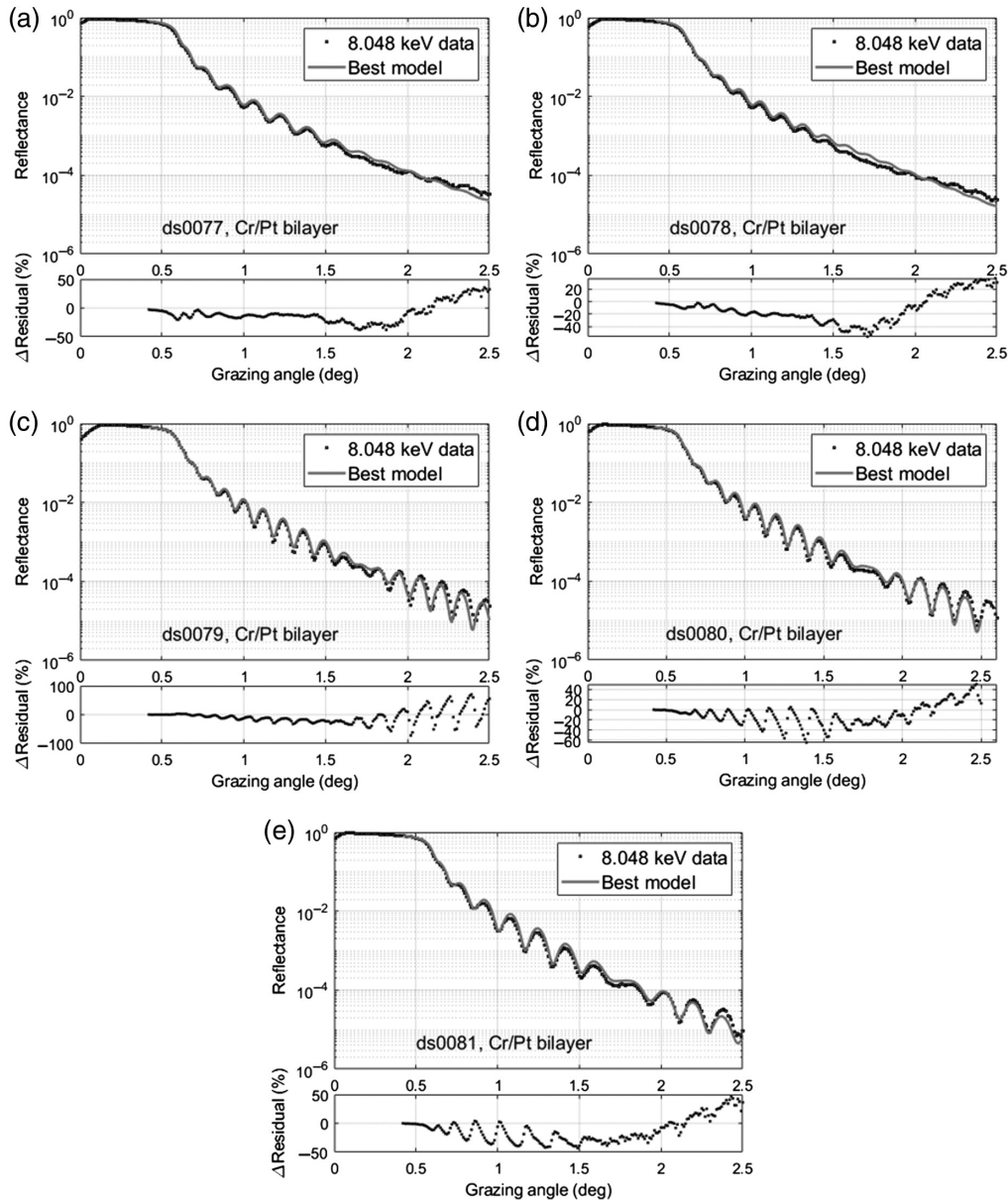
Fig. 11 (a)–(e) 8.048 keV specular reflectivity measurements of the BEaTriX reference coating samples, ds0077 to ds0081, including the best-fit model. Table 3 includes the fitted model parameters.

and that there is no indication of performance degradation due to the deposited coating as measured at 1.487 or 4.511 keV.

5 Summary

We have successfully coated the 456-mm-long mirror used in the BEaTriX facility, located at the INAF-OAB (Merate, Italy). We investigated the specular and nonspecular reflectance in single-layer Pt films and Cr/Pt bilayer films deposited on smooth Si substrates using DC magnetron sputtering at DTU Space. We evaluated the effect of nonuniformity in the 456-mm-long mirror and the effect on the Pt surface roughness when introducing Cr as an adhesive layer. We derived the thin film properties, including thickness, density, and roughness, utilizing x-ray reflectometry at 1.487 and 8.048 keV.

Table 3 Fitted model parameters of the 8.048 keV specular reflectivity measurements of the BEaTriX reference coating samples. Figure 11 includes the measured data and fitted model. The sample positions are illustrated in Fig. 5.

Sample ID	Energy (eV)	Layer	Composition	Thickness (nm)	Density (g/cm^3)	Roughness (nm)
ds0077	8048	Intermediate 3	Pt	**22.6**	21.5^c	**0.42**
		Intermediate 2	Cr	**3.51**	7.19^c	**1.06**
		Intermediate 1	SiO$_2$	2.0^c	2.65^c	0.74^b
		Substrate	Si	—	2.33^c	0.74^b
ds0078	8048	Intermediate 3	Pt	**27.8**	21.5^c	**0.45**
		Intermediate 2	Cr	**3.74**	7.19^c	**1.20**
		Intermediate 1	SiO$_2$	2.0^c	2.65^c	0.79^b
		Substrate	Si	—	2.33^c	0.79^b
ds0079	8048	Intermediate 3	Pt	**30.3**	21.5^c	**0.48**
		Intermediate 2	Cr	**4.05**	7.19^c	**0.66**
		Intermediate 1	SiO$_2$	2.0^c	2.65^c	0.31^b
		Substrate	Si	—	2.33^c	0.31^b
ds0080	8048	Intermediate 3	Pt	**27.5**	21.5^c	**0.48**
		Intermediate 2	Cr	**3.99**	7.19^c	**0.62**
		Intermediate 1	SiO$_2$	2.0^c	2.65^c	0.39^b
		Substrate	Si	—	2.33^c	0.39^b
ds0081	8048	Intermediate 3	Pt	**22.0**	21.5^c	**0.52**
		Intermediate 2	Cr	**3.93**	7.19^c	**0.68**
		Intermediate 1	SiO$_2$	2.0^c	2.65^c	0.54^b
		Substrate	Si	—	2.33^c	0.54^b

[a]Coupled parameters.
[b]Coupled parameters.
[c]Fixed values based on *a priori* assumptions (described in text).
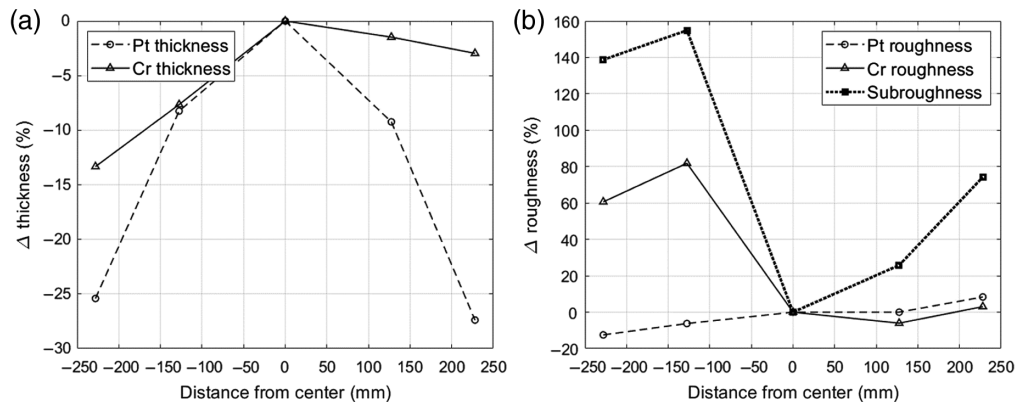[d]The parameters allowed to vary are presented in bold.

Fig. 12 The BEaTriX reference coating samples fitted coating (a) thickness and (b) roughness deviation relative to the center sample ds0079. The fitted model parameters are shown in Table 3.

The results showed that a thin intermediate layer of Cr decreases the nonspecular reflectance in the Pt surface, which agrees with the results from the INAF-OAB technical report. The tape test of the Pt single layer displayed a visible residual, whereas the Cr/Pt bilayers proved to withstand the removal of the tape. These results favor the Cr/Pt bilayer mirror coating design. After coating the 456-mm parabolic mirror with a Cr/Pt bilayer, a reference coating was produced. We identified a Pt thickness nonuniformity of 28% from the center to edge of the 456-mm mirror, due to the effect of varying the distance between the sputtering target and sample surface. This does not affect the performance of the BEaTriX facility because it operates below the critical angle of Pt. A roughness nonuniformity was observed on the reference coating due to presputtering, the increased TSD, and increasing angle of incidence of the sputtered particles onto the substrate. However, it was reported by Vecchi et al.[9], that the parabolic mirrors surface roughness slightly decreased after coating and that there was no indication of performance degradation due to the deposited coating at 1.487 or 4.511 keV.

Though not necessary for the BEaTriX facility, the nonuniformity can be improved by utilizing a cathode power gradient or ring rotation speed gradient. The use of a ring rotation speed gradient will be tested in the coming months, as a new step motor that can produce a controlled ring speed gradient is currently being installed at the DTU Space coating facility. Furthermore, presputter shields and longer butterfly-wing collimators will be installed to remove contamination attributed to the presputtering and to limit the solid angle of sputtered particles.

References

1. D. Spiga et al., "Performance simulations for the ground-based, expanded-beam x-ray source BEaTriX," *Proc. SPIE* **11837**, 118370O (2021).
2. B. Salmaso et al., "Building the BEaTriX facility for the ATHENA mirror modules X-ray testing," *Proc. SPIE* **11822**, 118220M (2021).
3. S. Basso et al., "First light of BEaTriX, the new testing facility for the modular x-ray optics of the Athena mission," *A&A* **664**, A173 (2022).
4. "Italian national institute for astrophysics, Brera Astronomical Observatory," http://www.brera.inaf.it (accessed 17 December 2021).
5. M. Collon et al., "Silicon pore optics x-ray mirror development for the Athena telescope," *Proc. SPIE* **11822**, 1182206 (2021).
6. I. Ferreira et al., "ATHENA reference telescope design and recent mission level consolidation," *Proc. SPIE* **11822**, 12–31 (2021).
7. M. J. Collon et al., "X-ray mirror development and production for the Athena telescope," *Proc. SPIE* **11852**, 831–841 (2021).
8. B. Salmaso et al., "BEaTriX (Beam Expander Testing X-ray facility) for testing ATHENA's SPO modules: advancement status," *Proc. SPIE* **11180**, 1118026 (2019).
9. G. Vecchi et al., "Manufacturing and testing of the X-ray collimating mirror for the BEaTriX facility," *Proc. SPIE* **11822**, 118220N (2021).
10. N. F. Brejnholt et al., "NuSTAR on-ground calibration: II. effective area," *Proc. SPIE* **8443**, 84431Y (2012).
11. A. Furuzawa et al., "The current status of ASTRO-H/HXT development facility," *Proc. SPIE* **7437**, 79–86 (2009).
12. M. Todeschini et al., "Influence of Ti and Cr adhesion layers on ultrathin Au films," *ACS Appl. Mater. Interfaces* **9**(42), 37374–37385 (2017).
13. S. Cozma et al., "Characterization of platinum-based thin films deposited by thermionic vacuum arc (TVA) method," *Materials* **13**(7), 1796 (2020).
14. A.-C. Probst et al., "Coating stress analysis and compensation for iridium-based x-ray mirrors," *Appl. Opt.* **57**, 8775–8779 (2018).
15. A. Vickery et al., "Collimated magnetron sputter deposition for mirror coatings," *X-ray Opt. Instrum.* **2008**, 792540 (2008).
16. J. Dalla Torre et al., "Microstructure of thin tantalum films sputtered onto inclined substrates: experiments and atomistic simulations," *J. Appl. Phys.* **94**(1), 263–271 (2003).
17. A. Dirks and H. Leamy, "Columnar microstructure in vapor-deposited thin films," *Thin Solid Films* **47**(3), 219–233 (1977).

18. N. Brejnholt, "NuSTAR calibration facility and multilayer reference database: optic response model comparison to NuSTAR on-ground calibration data: optic response model comparison to NuSTAR on-ground calibration data," PhD thesis (2012).
19. S. Massahi et al., "Balancing of residual stress in thin film iridium by utilizing chromium as an underlayer," *Proc. SPIE* **11444**, 114444N (2021).
20. S. Massahi, *Industrialization of the Mirror Plate Coatings for the ATHENA Mission*, Technical University of Denmark (2019).
21. P. L. Henriksen et al., "Qualification and performance of the low-energy x-ray reflectometer (LEXR)," *Proc. SPIE* **11444**, 114444J (2020).
22. M. Krumrey and G. Ulm, "High-accuracy detector calibration at the PTB four-crystal monochromator beamline," *Nucl. Instrum. Methods Phys. Res. Sect. A: Accel. Spectrom. Detect. Assoc. Equip.* **467–468**, 1175–1178 (2001).
23. N. C. Gellert et al., "Optimization of multilayer coatings for future high-energy focusing telescopes," *Proc. SPIE* **12181**, 121814K (2022).
24. Center for X-ray Optics, https://henke.lbl.gov/optical_constants/asf.html (accessed 1 June 2021).
25. S. Massahi et al., "Investigation of boron carbide and iridium thin films, an enabling technology for future x-ray telescopes," *Appl. Opt.* **59**(34), 10902–10911 (2020).
26. D. Spiga, B. Salmaso, and G. Vecchi, "Coating samples for the BEaTriX mirrors: surface roughness analysis," INAFOAB, internal report 01/2021 (2021).
27. Center for X-ray Optics, https://henke.lbl.gov/optical_constants/pert_form.htmll (accessed 1 June 2021).

Biographies of the authors are not available.